



OVERDUE FINES:

25¢ per day per item

RETURNING LIBRARY MATERIALS:

Place in book return to remove
charge from circulation records

STUDIES ON THE HEMOLYSIS KINETICS OF
HUMAN ERYTHROCYTES BY USING
A STOP FLOW SYSTEM

By

Chauying Jack Jen

A THESIS

Submitted to
Michigan State University
in partial fulfillment of the requirements
for the degree of

MASTER OF SCIENCE

Department of Mechanical Engineering

1980

ABSTRACT

STUDIES OF THE HEMOLYSIS KINETICS OF HUMAN ERYTHROCYTES BY USING A STOP FLOW SYSTEM

By

Chauying Jack Jen

A stop flow system has been designed to obtain information concerning cellular damage. Human erythrocytes were chosen as a biological model system for studying the damage kinetics. The experimental technique presently developed enables the continuous monitoring of hemolysis kinetics with good precision and the short time kinetic data are accessible. The kinetics of hemolysis, induced by hypotonic or hypertonic perturbations are investigated. The hemolysis kinetics are characterized by a lag time, a rapid initial rate, followed by transition to a slower rate. The influence on hemolysis kinetics by injection rates as well as blood storage time has been studied. The results of this work are significant by direct transfer of knowledge from engineering design to clinical applications.

Dedicated to My Wife and Daughter

ACKNOWLEDGEMENTS

I would like to express my deepest appreciation to my major advisor, Dr. John J. McGrath, for his patient guidance and support throughout this work.

Special thanks to Dr. John Brighton who introduced me to the field of biomedical engineering. Thanks also to Dr. D. K. Anderson, Dr. J. F. Foss, and many people in the Department of Mechanical Engineering for helping me with my training in engineering.

My sincere appreciation to my parents whose life long love and encouragements sustained me these many years.

I would like to express my gratitude to my mother-in-law who helped me during the time of the greatest need.

TABLE OF CONTENTS

	Page
LIST OF FIGURES	v
Chapter	
I. INTRODUCTION	1
Background	2
II. MATERIAL AND METHODS	10
Sample Preparation	10
Hemolysis Determination	11
Principles for the Measurement of Hemolysis	
Kinetics	12
The Experimental Apparatus	12
III. THE CHARACTERISTICS OF THE SYSTEM	17
Calibration for Percent Hemolysis as a Function	
of Normalized Photocell Voltage	17
The Hematocrit Effect	18
The Optical Transients	20
The Cell Volume Effect	23
IV. RESULTS	28
Characteristic Signal Outputs for Hemolysis	
Kinetics	28
Hemolysis Kinetics of Erythrocytes	30
The Effect of Shear on Hemolysis	36
The Effect of Storage Time on Hemolysis Kinetics .	38
V. DISCUSSION	42
Suggestions for Future Work	47
REFERENCES	50

LIST OF FIGURES

Figure	Page
1. Schematic representation of relation between NaCl concentration and volume/shape of red cells	4
2. Survival curves for various cell types.	6
3. Schematic representation of the hemolysis process . .	8
4. Schematic representation of the experimental apparatus	13
5. Schematic representation of the mixer and the test cell	14
6. Calibration curve for percent hemolysis as a function of normalized photocell voltage	19
7. Normalized photocell voltage as a function of sample hematocrit	22
8. Hemolysis-independent optical transients as a function of sample hematocrit	24
9. Normalized photocell voltage as a function of NaCl concentration for 10% hematocrit samples	26
10. Typical photocell voltage outputs as a function of exposure time	29
11. Hemolysis kinetics at ambient temperature	31
12. Correlations of initial hemolysis rate as a function of water activity	33
13. Proposed flow pattern in the mixer	37
14. Effect of injection rate on hemolysis kinetics . . .	39
15. Effect of blood storage time on hemolysis kinetics .	41

CHAPTER I

INTRODUCTION

The present research effort considers two important aspects of the dynamics of damage in living cellular systems. These aspects are: (a) the development and characterization of instrumentation for measuring the kinetics of damage and, (b) the use of such instrumentation in establishing a data base for ongoing modeling research. The dynamics of the destruction of human red blood cells have been chosen for examination. This choice is based on the fact that the human red cell is a well-documented biological system, making it an attractive model system, and that there are many clinical problems which would benefit from a clearer understanding of the sensitivity of the red cell to various external perturbations.

Previous research had demonstrated that experimental data for short times were necessary for modeling of cell damage and that these data were accessible using a modified stop flow technique. It was also apparent that potential interfering factors would be observed under some conditions. Therefore, the aim of the present work was to construct a stop flow system and to investigate these interfering factors with the aim of minimizing or eliminating it. The improved device was then to be used to determine various characteristics of red cell hemolysis kinetics. In particular,

experimental data were desired which could be used for comparing the nature of hypertonically and hypotonically-induced hemolysis as well as the effect of cell storage on the damage sensitivity for both modes of perturbation.

Background

The blood functions mainly as a medium for maintaining a suitable and nearly constant environment for the growth and function of the innumerable cells of the body. It also serves as a medium for transport of mass and energy between the external environment and the various tissues of the body. Whole blood can be divided into about 55 vol % plasma, and about 45 vol % cells. The plasma portion of the blood is essentially a dilute (0.154 M or 0.9 w/v %) electrolyte solution containing about 8 wt % proteins. The circulating cell population consists of about 95% (by number) red blood cells, or erythrocytes. White cells and platelets comprise the remaining 5%.

The primary function of the circulating red cells is to maintain in the circulation the high concentration of hemoglobin essential for the transport of the large amount of O_2 and CO_2 necessary for respiration. As the physical solubility of O_2 and CO_2 in blood plasma is rather low, the requirements for their transport are met by the reversible binding of O_2 and CO_2 with the hemoglobin contained in the red blood cells. The red cell normally has the shape of a biconcave disc which can deform and can pass through small capillaries without being irreversibly altered. Normally the

red cell membrane is very permeable to water but not ions. Because of the deformability and selective permeability of the membrane the red cell volume and shape changes according to the tonicity of the extracellular solution. A schematic presentation of the relation between tonicity and volume/shape of red cells is shown in Figure 1 (1). In hypertonic solutions, the cell volume becomes smaller and the cells become flatter. In hypotonic solutions the cell volume increases and the shape of the cell approaches that of a sphere. Any further changes in volume induced by osmotic perturbation results in lysis, i.e., structural changes permitting leakage of hemoglobin. The integrity of the red cell seems to depend on there being a state of order among the components which make up the membrane structure. When this state of order is sufficiently disturbed, hemoglobin is lost and the cell hemolyzes (2).

Hemolysis is generally considered to be an instantaneous and all-or-none event once the "critical point" is reached (3,4). The standard technique employed for hemolysis determination involves centrifugation, cell lysing, hemoglobin fixation in a particular oxygenated state, and measurement of hemoglobin optical absorption (3). Since the minimum time needed to obtain the first hemolysis data in this manner is several minutes, an essential portion of the hemolysis dynamics close to time zero is inaccessible using this procedure. Observations from a modified stop flow apparatus demonstrated that the intensity of a light beam passing through a column of partially hemolyzed red cells could be calibrated as a function of hemolysis (5). Therefore, the construction of such a

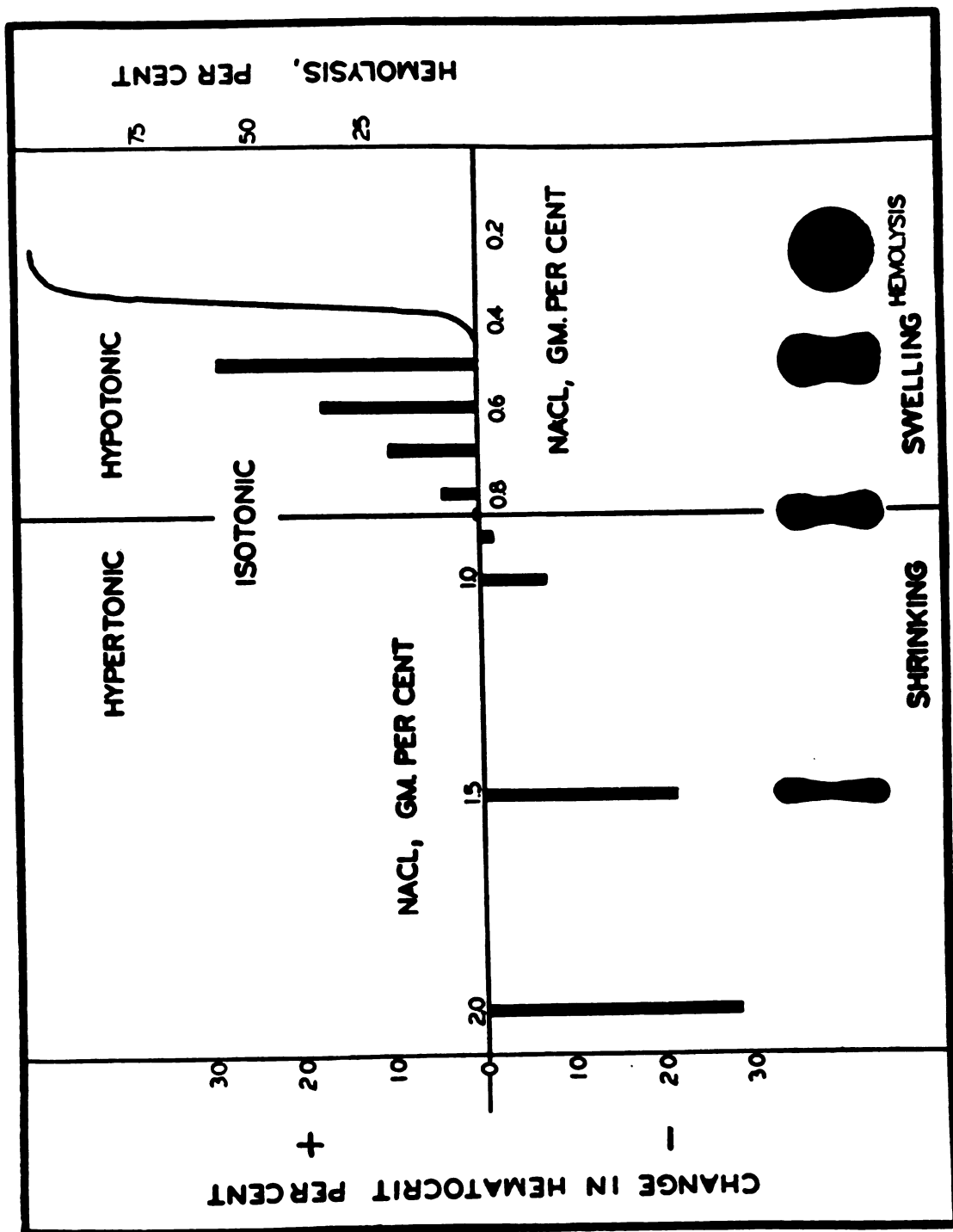


FIGURE 1.--Schematic representation of relation between NaCl concentration and volume/shape of red cells.

system will provide a sensitive and meaningful measure of damage kinetics as desired. Moreover, because of the medical importance previously discussed, the results of this work are significant by direct transfer of knowledge from engineering design to clinical applications.

One important application is the cryopreservation of biomaterials. Whole organ transplantation shows great promise as a surgical technique. But, this is only possible if donor organs are readily available. In order to develop successful long term storage techniques, it is essential to thoroughly understand the mechanism of cellular damage induced by the cryopreservation process. In an effort to reveal mechanistic detail, the effect of cooling rate (the rate of change of the sample temperature with respect to time) on cell survival has received quite intense attention. The cell survival, as a function of cooling rate, is generally an inverted U shape curve (6), which suggests that at least two competing phenomena are involved in determining ultimate survival. Figure 2 (provided by Dr. S. P. Leibo, Oak Ridge National Laboratory) shows this behavior for several cell types. The proposed dual mechanism hypothesis for freezing damage can be summarized as follows: at slow characteristic cooling rates (below the optimum cooling rate) the increased solute concentrations present during freezing and the longer exposure times are the dominant causes of cell damage. Survival can be improved by increasing the cooling rate but there is a limit to this

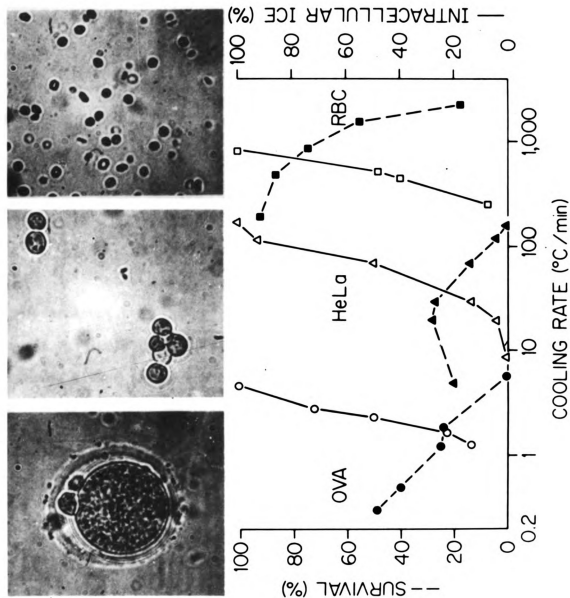


FIGURE 2.--Survival curves for various cell types.

enhancement since increasing the cooling rate will eventually cause intracellular ice formation and cell death.

Lovelock (7) demonstrated that freeze-thaw hemolysis of red blood cells suspended in normal saline could be duplicated by exposure to hypertonic saline solutions and redilution to isotonic concentrations. He discovered that there are three major modes of freeze-thaw damage at sub-optimal cooling rates.

1. Osmotic damage by exposure to hypertonic NaCl solutions.
2. Thermal shock damage, defined as exposure to a hypertonic solution followed by a temperature drop, not necessarily to freezing.
3. Posthypertonic hemolysis, experienced by cells suspended in hypertonic media which are then rediluted into isotonic media.

It is apparent that the first two modes in most cases are coupled and it is likely that all three are intimately related. The present research effort is focused on the osmotic damage.

McGrath (5) postulated a model for the kinetics and thermodynamics of red cell hemolysis. Lovelock (8) assumed that hypertonic solutions are capable of removing a sufficient amount of critical membrane components (lipids) so that the cell becomes increasingly permeable to solutes, eventually large molecules such as hemoglobin will leave the cell--"Membrane Dissolution Theory." Since the characteristic times associated with hemoglobin diffusing through the cell are short compared with the release of lipid, the hemolysis process can be modeled by a lipid diffusion rate-limited process causing a critical state to be attained, followed by a very rapid release of hemoglobin (see Figure 3). The intracellular

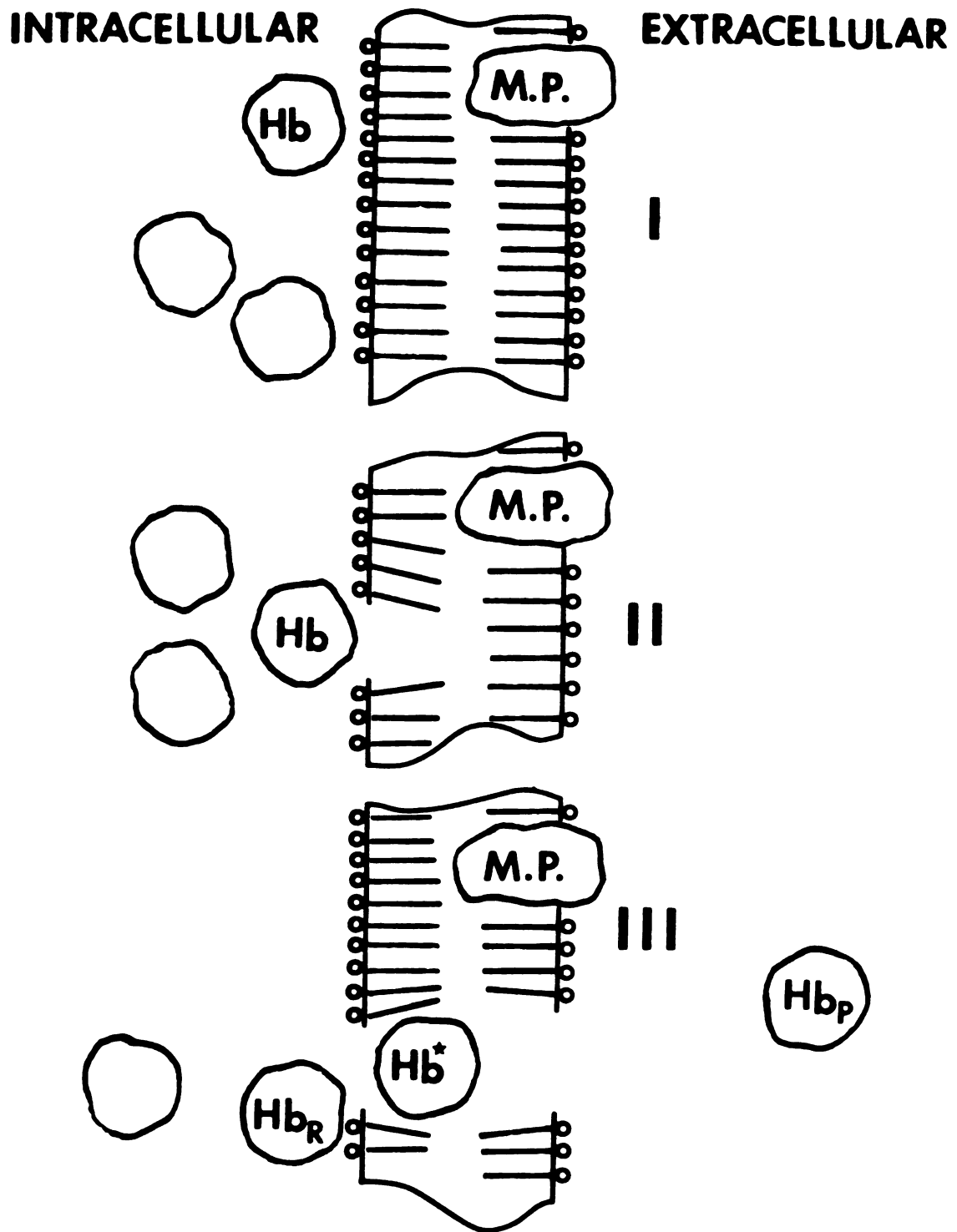
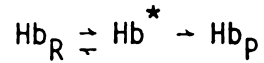


FIGURE 3.--Schematic representation of the hemolysis process.

hemoglobin molecules are the reactant molecules Hb_R , the molecules in the process of passing through the membrane are in the activated state Hb^* , and those in the extracellular medium are "product" molecules Hb_P . The reaction can be expressed as



and the reaction rate as

$$\frac{-d[\text{Hb}_R]}{dt} = [\text{Hb}_R] \cdot \nu \cdot \exp\left[\frac{-\Delta G_{\text{Hb}}^{\circ'}}{KT}\right]$$

Therefore, the studies on hemolysis kinetics will provide an invaluable data base for understanding the mechanism of hemolysis as well, by providing information on relevant activation energies such as $-\Delta G_{\text{Hb}}^{\circ'}$ shown above.

CHAPTER II

MATERIAL AND METHODS

Sample Preparation

Whole venous blood was obtained in EGTA tubes collected by standard procedures at the American Red Cross, Lansing Blood Bank. All of the blood not used at the day of collection was stored in its own plasma at 4°C. If not used within two days after collection the blood was discarded unless the blood was destined to be used for the experiments testing the effect of storage time on hemolysis kinetics. Erythrocytes were washed twice in unbuffered normal saline (0.9% w/v) immediately before use. The standard washing procedure employed is described as follows. Cells were gravity-settled at the bottom of tubes without centrifugation. This procedure yields two distinct zones separated by a boundary above which was the plasma volume. Both the supernatant and the "buffy-coat" layer (containing white cells) atop the erythrocytes were gently removed by a pasteur pipette. Normal saline prepared in distilled water was added to fill the tubes and the cells were resuspended by inverting the capped tubes several times. The sample was centrifuged at the maximum speed of a clinical centrifuge for 12 minutes. The supernatant was pipetted out. The washing cycle was repeated once and the final supernatant decanted was clear. Normally, the hematocrit of the packed cells was measured

to be 85%-95% after the centrifugation. Two to four tubes of blood were combined and used for each set of hemolysis kinetics experiments. These experiments were completed within about three hours after cell washing. Washed cells were never restored for the next day's experiments because they showed significant auto-hemolysis after storing overnight in the refrigerator (in normal saline).

Hemolysis Determination

Hemolysis by definition is the release of the oxygen-binding protein, hemoglobin, from within the erythrocytes to the extracellular medium. The extent of hemolysis can be determined by measuring the ratio of the hemoglobin present in the supernatant (extracellular space) per unit volume and the total hemoglobin (both intra- and extracellular hemoglobin) per unit volume. The standard technique employed for hemolysis determination was similar to that of Zade-Oppen's (3). Hycel cyanmethemoglobin reagent (5 ml) was placed in a previously blanked tube (Bausch and Lomb Spectronic 20 test tubes). One hundred μ l of blood (10% hematocrit) was added to the tube and mixed well. After 10 minutes of reaction time this tube was then placed in the Spectronic 20 spectrophotometer and the absorbance at 540 nm was recorded as A_t . The rest of the blood sample was centrifuged to pellet the intact cells. One hundred μ l of the supernatant was mixed with the same amount of reagent mentioned above and the supernatant absorbance, A_s , was measured. Hemolysis was then calculated using the following equation

$$\%H = \frac{A_s}{A_t}$$

and was not corrected for the volume percentage occupied by the cells.

Principles for the Measurement of Hemolysis Kinetics

The intact, healthy erythrocytes are very effective in scattering light. They appear as bright objects under a phase-contrast light microscope. As the cells hemolyze, they are much less effective in scattering light. These hemolyzed cells appear almost transparent under a microscope and hence are called "ghosts." Therefore, the intensity of a transmitted light beam through a homogeneous red cell suspension provides a very sensitive measure of the extent of hemolysis. As the hemolysis progresses within the cell population there is an increase of transmitted light intensity. When a calibration between the extent of hemolysis and the light intensity is established, the hemolysis kinetics can be obtained by continuously monitoring the light intensity changes. However, an analytical approach to light scattering from deformable living cells is limited at the present time (9).

The Experimental Apparatus

The major components of the experimental apparatus are shown in Figure 4 and Figure 5. The light source was a 6-volt tungsten microscope illuminator which was powered by a Sorensen Nobatron T50-1.5 D.C. power supply. The incident light intensity

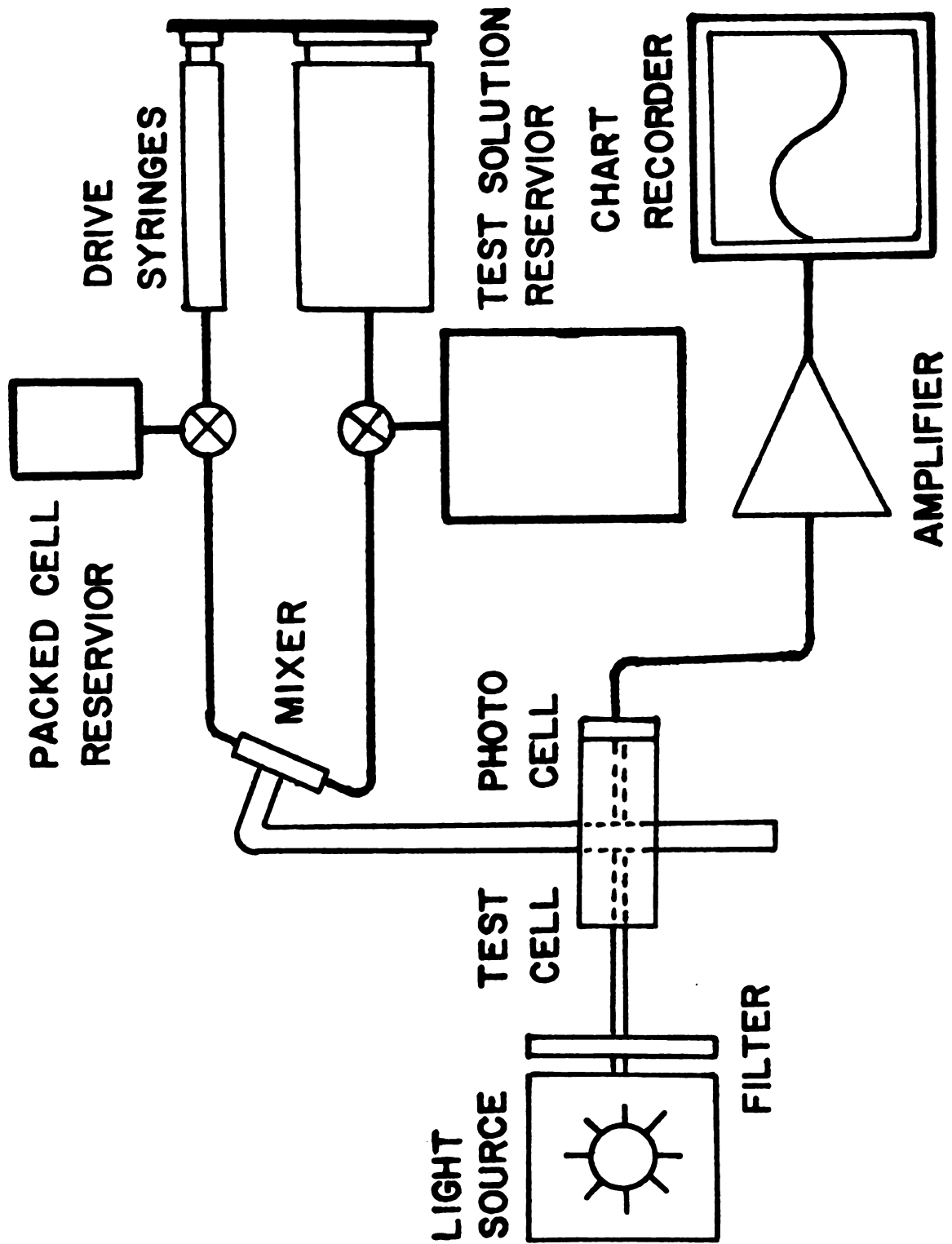


FIGURE 4.--Schematic representation of the experimental apparatus.

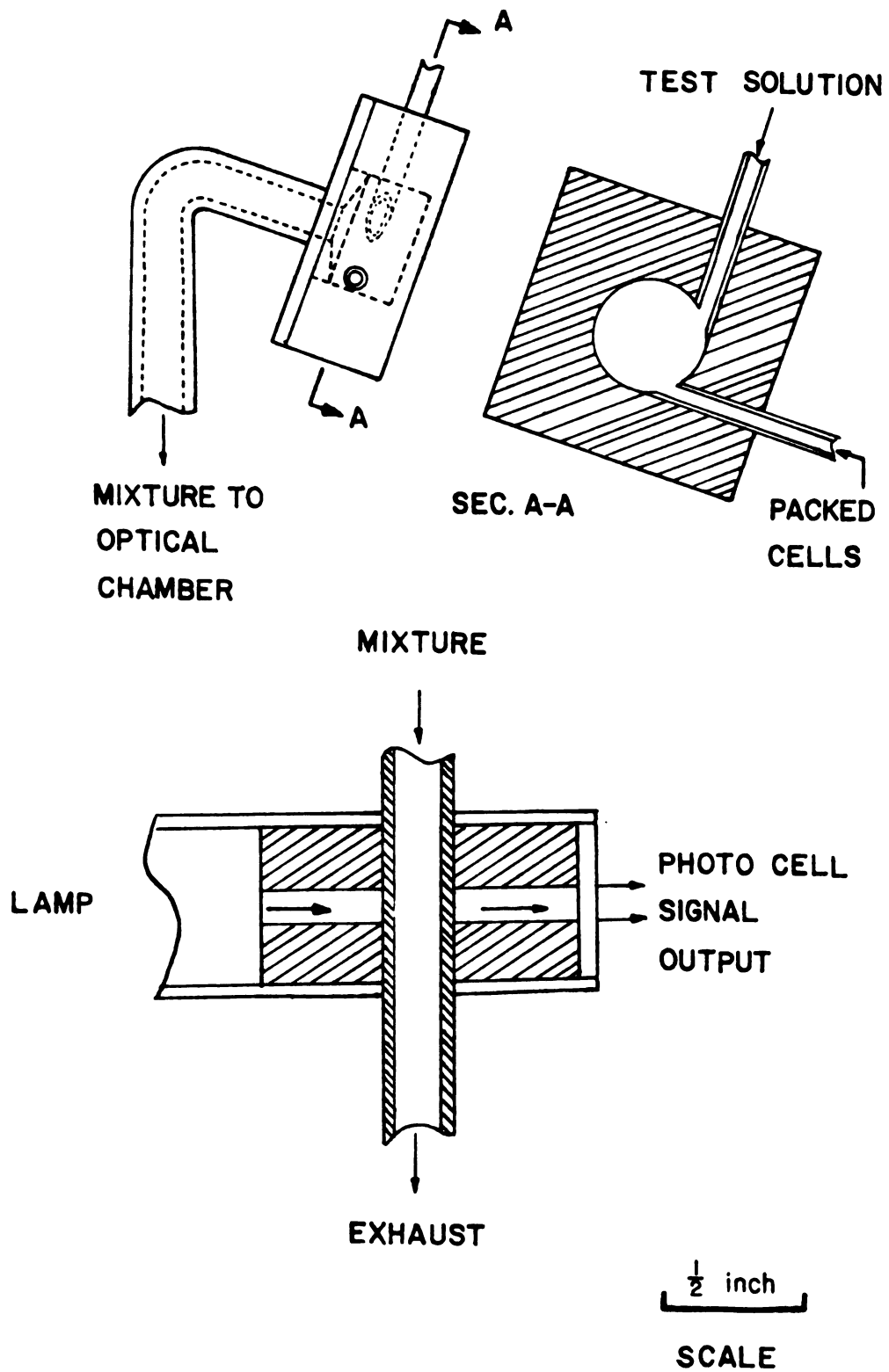


FIGURE 5.--Schematic representation of the mixer and the test cell.

to the cell suspension was adjusted either by the power-supply voltage or through a diaphragm mounted within the lamp housing. A glass tube (I.D. 3.2 mm, O.D. 5.4 mm) served as the test chamber. The distances above and below the observation point were 10 cm and 5 cm respectively. The incident light beam passed through a 2.4 mm diameter channel, reached the observation point, and the forward transmitted light was monitored by a photocell. The photocell output voltage was amplified and high frequency noise was filtered by a circuit described in reference (5). The final output voltage was displayed on an Esterline-Angus Speed Servo II strip chart recorder.

The injection system consisted of two plastic drive syringes, with volumes of 10 ml (test solution syringe) and 1 ml (packed cell syringe) respectively. The area ratio of these two syringes was 9:1. For the coupled drive configuration shown in Figure 4, with equal stroke lengths for both plungers, the final mixture hematocrit was calculated to be between 8.5% and 9.5% (depends on the hematocrit of packed cells loaded). The packed cell reservoir was constructed from a 10-ml syringe held upright above a three-way valve. A flask located on the bench contained the test solution. Tygon tubing was used for connections, because it could be bent easily and was transparent (good for trouble shooting). The length and size of this tubing were kept at a minimum to reduce the "dead volume" and hence make efficient use of the valuable blood. A detailed analysis concerning the blood flow conditions in various parts of the system is presented in Chapter IV.

A mixture was designed to provide rapid and complete mixing. Packed cells and the test solution were tangentially injected into the disc-like mixer. The solution inlet was 90° behind the cell inlet. The mixed cell suspension was then delivered into the test chamber which was held vertically, parallel to the direction of cell sedimentation, to assure a constant cell density at the observation point (5,10). In order to prevent the unmixed blood from getting into the test chamber, the blood inlet was at the bottom part of the mixture and the outlet was at an angle about 30° up.

CHAPTER III

THE CHARACTERISTICS OF THE SYSTEM

The system was very stable when the test chamber was filled with isotonic saline, in the presence or absence of red cells. With constant illumination from the tungsten lamp the photocell output voltage remained constant with less than 1% variation for a period of two hours. A calibration curve was constructed to convert the light intensity (voltage output) to the extent of hemolysis. However, in general there are potentially interfering factors unrelated to hemolysis, which can influence the signal output. These factors are discussed in the following sections.

Calibration for Percent Hemolysis as a Function of Normalized Photocell Voltage

Cells washed with normal saline were packed and divided into two tubes. Samples from tube 1 were hemolyzed by one of three ways: hypertonic exposure, hypotonic exposure, or freeze-thaw damage. Samples from tube 2 were not induced to hemolyze. The cell density and saline concentration were then adjusted to be 10% and 0.9% NaCl respectively, for both tubes. Different proportions of these two cell suspensions were mixed to get a wide range of hemolysis. Both voltage output and hemolysis were determined for

individual samples according to the methods described as $\bar{V} = V_{\text{test}}/V_{0\%H}$, where $V_{0\%H}$ is the base line voltage for 0% hemolysis sample. The results were plotted as \bar{V} vs $(1 - \frac{\%H}{100})$ in Figure 6. The best exponential fit appears as

$$\bar{V} = (1 - \frac{\%H}{100})^{-1.25}, \text{ or } \%H = 100(1 - \bar{V}^{-0.8})$$

with the correlation coefficient of $r^2 = 0.985$. No significant differences were found among cells hemolyzed by the three different treatments, indicating that for the present case a hemolyzed cell is a hemolyzed cell, invariant to the method of production.

The Hematocrit Effect

Suspensions with higher hematocrit substantially reduce the intensity of transmitted light. This hematocrit effect is shown in Figure 7. The photocell voltage was normalized with respect to the 10-volt reference voltage which was derived from a cell-free, normal saline sample. This normalized voltage appeared to change inversely with the sample hematocrit in the hematocrit range from 1% to 20%. Therefore, a source of inaccuracy could be in the non-reproducible delivery of cells from the syringe pair. This factor was checked. There was a $\pm 1.5\%$ variation about the mean signal value for the non-hemolyzed cells suspended in the isotonic saline. This represents the inaccuracy produced by the delivery system. It was known that different samples of packed cells, prior to the delivery, were of different hematocrit ranging from 85% to 95%. This difference in packness could produce an inaccuracy of about $\pm 7\%$ in the signal value.

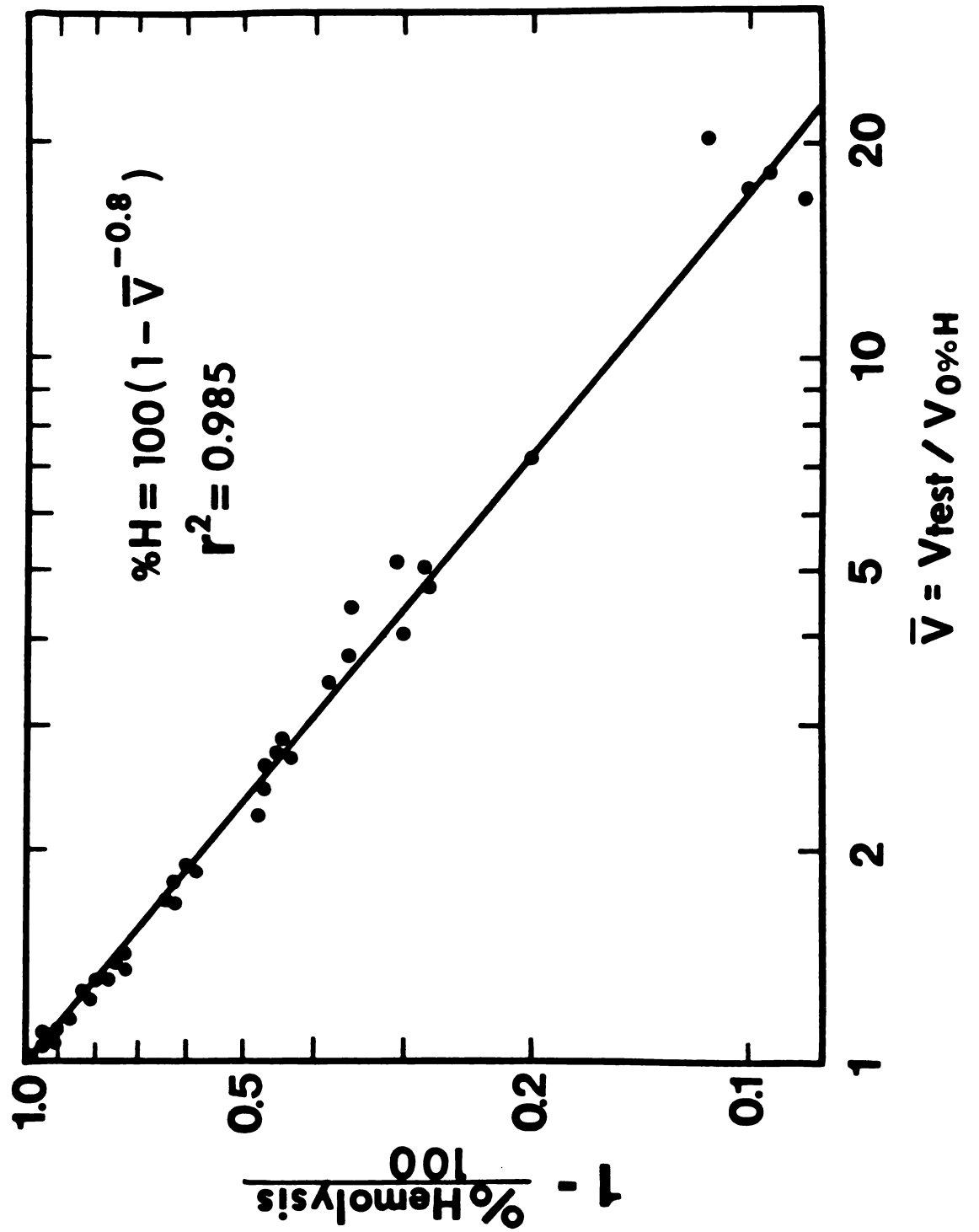


FIGURE 6.--Calibration curve for percent hemolysis as a function of normalized photocell voltage.

All of these variations would influence the $V_{0\%}$ values. However, earlier results with a different but similar device demonstrated that the \bar{V} values were unchanged among samples of the same extent of hemolysis but with different hematocrits (5). Therefore these variations do not effect the hemolysis measurements.

The Optical Transients

Although the system characteristics described thus far indicate that the desired hemolysis data can be measured, there is a major weakness in such a stop flow system. Earlier investigators reported transient variations in absolute signal value within the first 30 seconds after flow was stopped (5,11). Since this transient signal variation was observed with cell suspensions premixed with isotonic saline, it did not reflect the degree of hemolysis nor was it due to the effect of mixing between two different solutions. Because of this artifact the determination of the 0% hemolysis signal output used for normalization was seriously impaired. As a consequence the kinetic information of hemolysis would be distorted since this transient signal variation could not be diminished by taking \bar{V} , the ratio of V_{test} and $V_{0\%}$, as the parameter representative of hemolysis. One of the major tasks of this work was to find a way to either minimize or remove this artifact. Various factors, including the dimensions and material of the test chamber, the size of the light channel, the location of the photocell, etc., were investigated and generally no minimization of the optical transients was obtained. It was concluded that

optical transients were not associated with the geometry of the system per se, but might be related to the cell-flow interactions. Under non-flow conditions the voltage output of a homogeneous non-damaged cell suspension should not give any transient signal variations. On the other hand, a rapid and complete mixing was essential for fast kinetic studies. Hence the sample must be subjected to flow conditions. It was also clearly not desirable to add detergents or fixatives to the sample or solution since these reagents might influence the hemolytic response of cells.

Since the hematocrit is known to effect $V_{\text{cell}}/V_{\text{N.S.}}$ (Figure 7) and cell-cell interactions in flow situations, the effect of varying hemotocrits on the optical transients was investigated. The parameter $\Delta V/V_{\text{min}}$ was chosen as the measure of optical transients where ΔV was the maximum voltage variation within 30 seconds after flow cessation and V_{min} was the minimum voltage with the same time period. The results are shown in Figure 8. The values of $\Delta V/V_{\text{min}}$ could be as large as 15% or more for low (about 1%) hematocrit conditions. As the hematocrit was increased, both the mean value of $\Delta V/V_{\text{min}}$ and its variation were reduced dramatically. However, for samples with a hematocrit greater than 7.5%, the artifact remained consistently low and was no longer hematocrit-dependent. This low value artifact, about 1%, was probably due to the background noise generated from the system as a whole.

Based on the following considerations, values of 8.5% - 9.5% were chosen for the hematocrit of the final reaction mixture. The disadvantages of using higher hematocrit samples were: (1) more

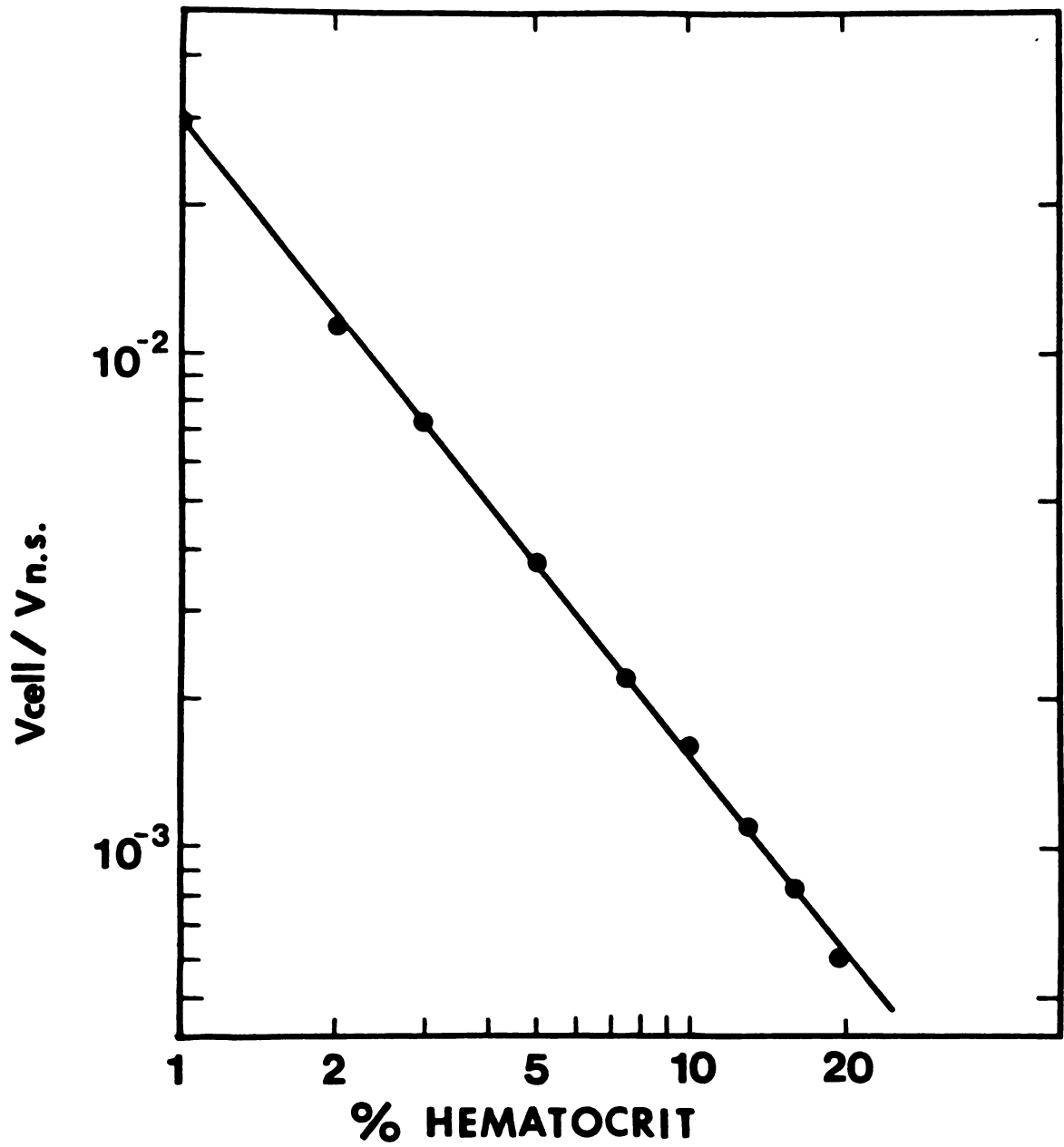


FIGURE 7.--Normalized photocell voltage as a function of sample hematocrit.

blood and prolonged sample preparation time were necessary to perform the same experiments; (2) the actual NaCl concentration of the reaction mixture deviated from that of the test solution because of the relatively large values of the cell/test solution volume ratio; (3) the voltage output of the non-hemolyzed cell suspension, $V_{0\%H}$, was small enough at standard operating conditions such that it was seriously affected by the background noise or the "dark current." On the other hand, the shortcomings for using lower hematocrit samples were: (1) the system became less sensitive to hemolysis since $V_{0\%H}$ increased and consequently $V_{cell}/V_{N.S.}$ seemed to be a limiting factor (Figure 7) and the maximum optical gain in the system would be reduced; (2) more importantly, the optical transients mentioned above would introduce large experimental errors as shown in Figure 8.

The Cell Volume Effect

It is known that the intracellular water mass, hence the cell volume, varies with the surrounding NaCl osmolality (12). In the case of cells subjected to osmotic shock, the cell volume changes first and is followed by hemolysis. Once the cell volume changes, the index of refraction of the cell also changes and subsequently alters the amount of light transmitted through the cell suspension. More light is scattered by the high refractive-index cells which are suspended in hypertonic solution. Minimum cell volume is reached when cells are subjected to salt concentrations equal to or above 1M (12). A normalized voltage defined as the ratio of

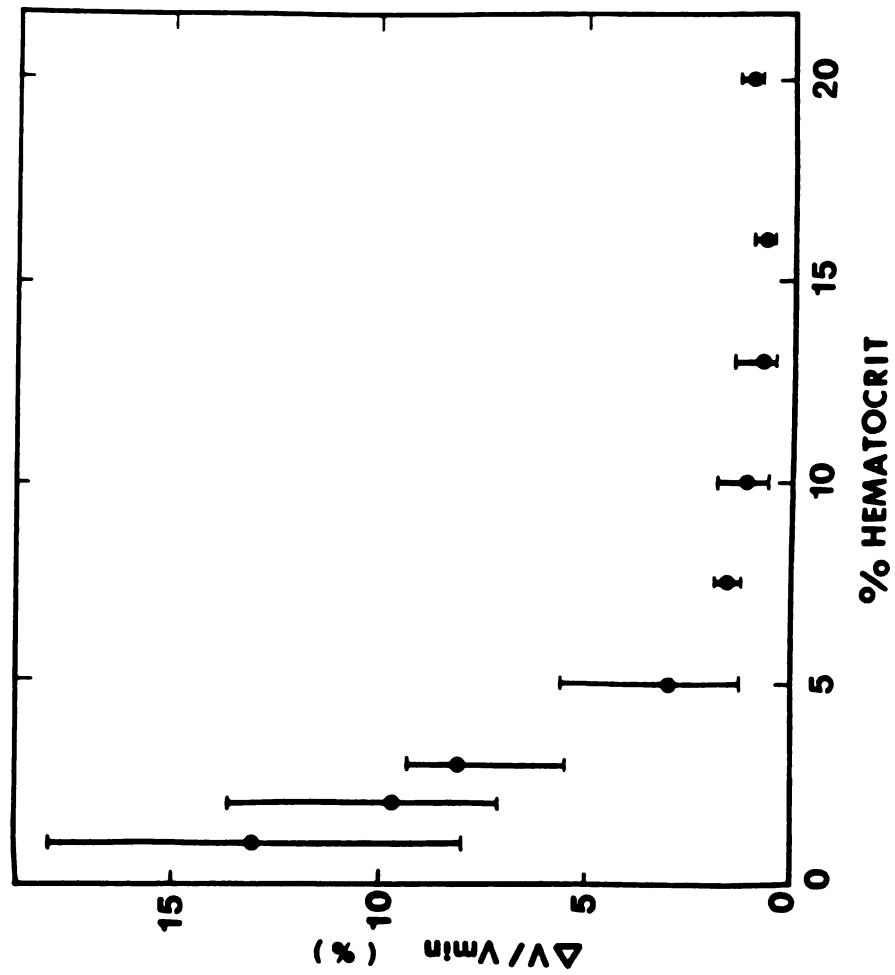


FIGURE 8.--Hemolysis-independent optical transients as a function of sample hematocrit.

$V_{0\%H}$ (minimum volume, no hemolysis) divided by the voltage of cells in normal saline is plotted as a function of test solution NaCl concentration (Figure 9). This curve reaches a constant level, about 60%, at 1M NaCl. For the hypertonic test solutions used in this work, $V_{0\%H}$ represented the voltage output from a minimum voltage sample and this voltage remains virtually constant over the concentration range from 1M to 4M NaCl. However, for cells subjected to hypotonic shock, the cell volume change was more difficult to determine. After the flow stopped, the signal does not reach a steady level "instantaneously." The signal performs a rapid increase which lasts for approximately 2 seconds. This initial signal increase is observed for all the hypotonic saline test solutions. For a 0.6% NaCl test solution, the signal reaches a steady level which is about 15% higher than the initial value (shown as an open circle in Figure 9). For test solutions with NaCl concentration less than 0.6% the signal is biphasic, i.e., a rapid change is followed by a subsequent increase with different slope. As determined by hemoglobin release test, there was no significant hemolysis when cells are mixed with 0.6% saline. It is known that the critical volume at which hypotonic hemolysis occurs is about 1.5 to 1.7 times the normal cell volume (2). Moreover, cells of critical volume are postulated to remain "intact" for a short time period, about 2 - 3 seconds, before hemolysis actually takes place (13). Therefore, the initial, rapid increase of the signal is not hemolysis-related but is probably due to the release of other

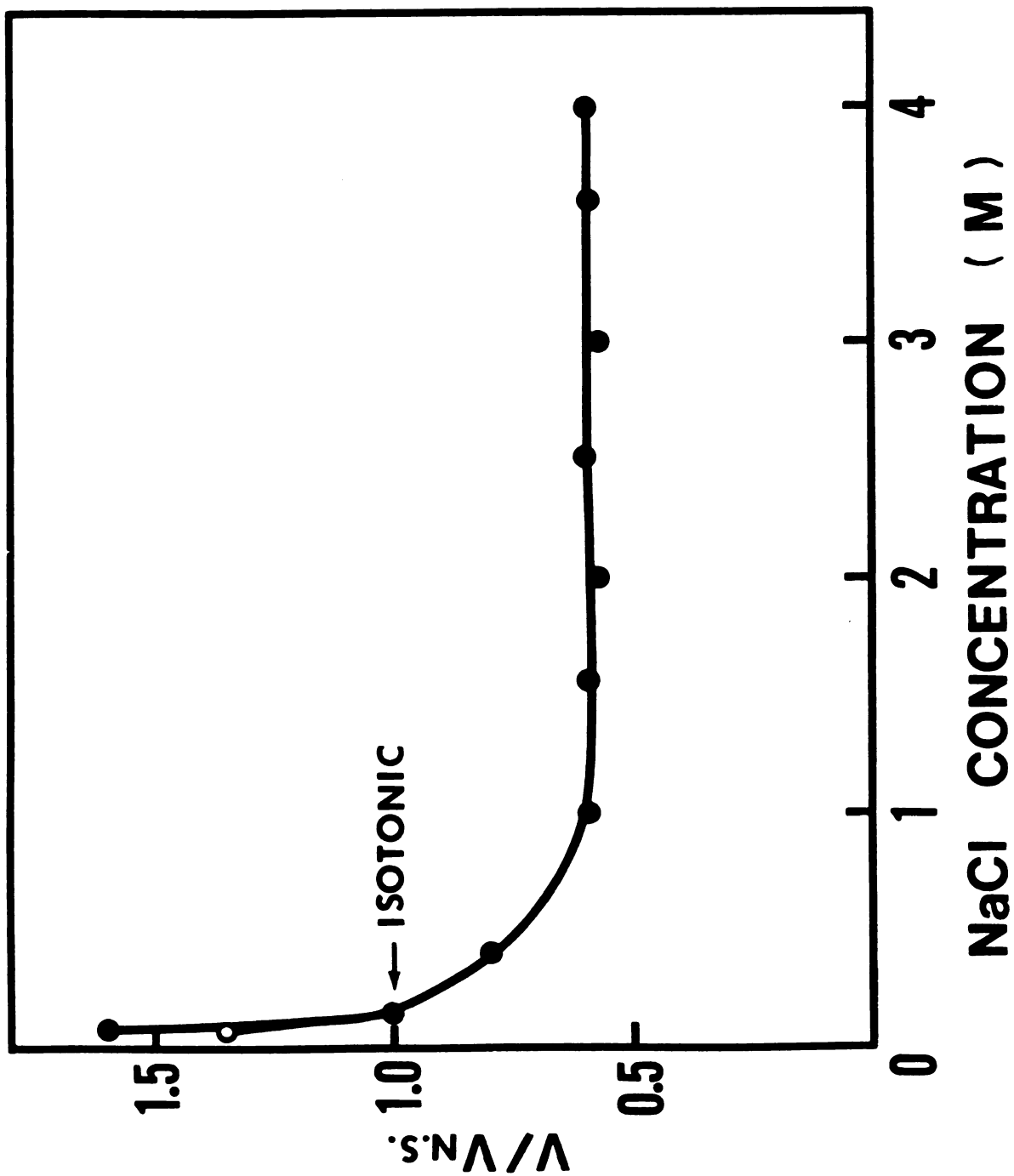


FIGURE 9.--Normalized photocell voltage as a function of NaCl concentration for 10% hematocrit samples.

cellular contents at critical volume. The steady state level of signal obtained from cells mixed with 0.6% NaCl test solution was taken as $V_{0\%H}$ for hypotonic normalization. This value was applied to other test solutions with NaCl concentrations less than 0.6%.

CHAPTER IV

RESULTS

Characteristic Signal Outputs for Hemolysis Kinetics

Packed cells and test solutions were mixed together and delivered into the test chamber at time zero. The signal outputs were continuously monitored by a strip chart recorder. All experiments were carried out at room temperature. Figure 10 shows typical examples of photocell signal outputs as a function of time for cells subjected to hypertonic (3 M NaCl) or hypotonic (0.077 M NaCl) exposure. In the case of hypertonic exposure, the cells reach minimum volume "instantaneously" (about 250 msec according to reference 11), so did the signal output. If the cells were not hemolyzing the signal would remain constant. In the present example, the signal gradually increases with time, which indicates that hemolysis is occurring. There is an apparent lag time before hemolysis starts. Furthermore, the hemolysis starts in a relatively rapid manner and gradually slows down. Eventually the hemolysis asymptotically reaches a maximum value where the signal no longer changes significantly. In the case of hypotonic exposure, the signal reaches a minimum value instantaneously but only remains at that level momentarily. A rapid signal increase, followed by a smooth increase represents the hemolysis process. The apparent lag

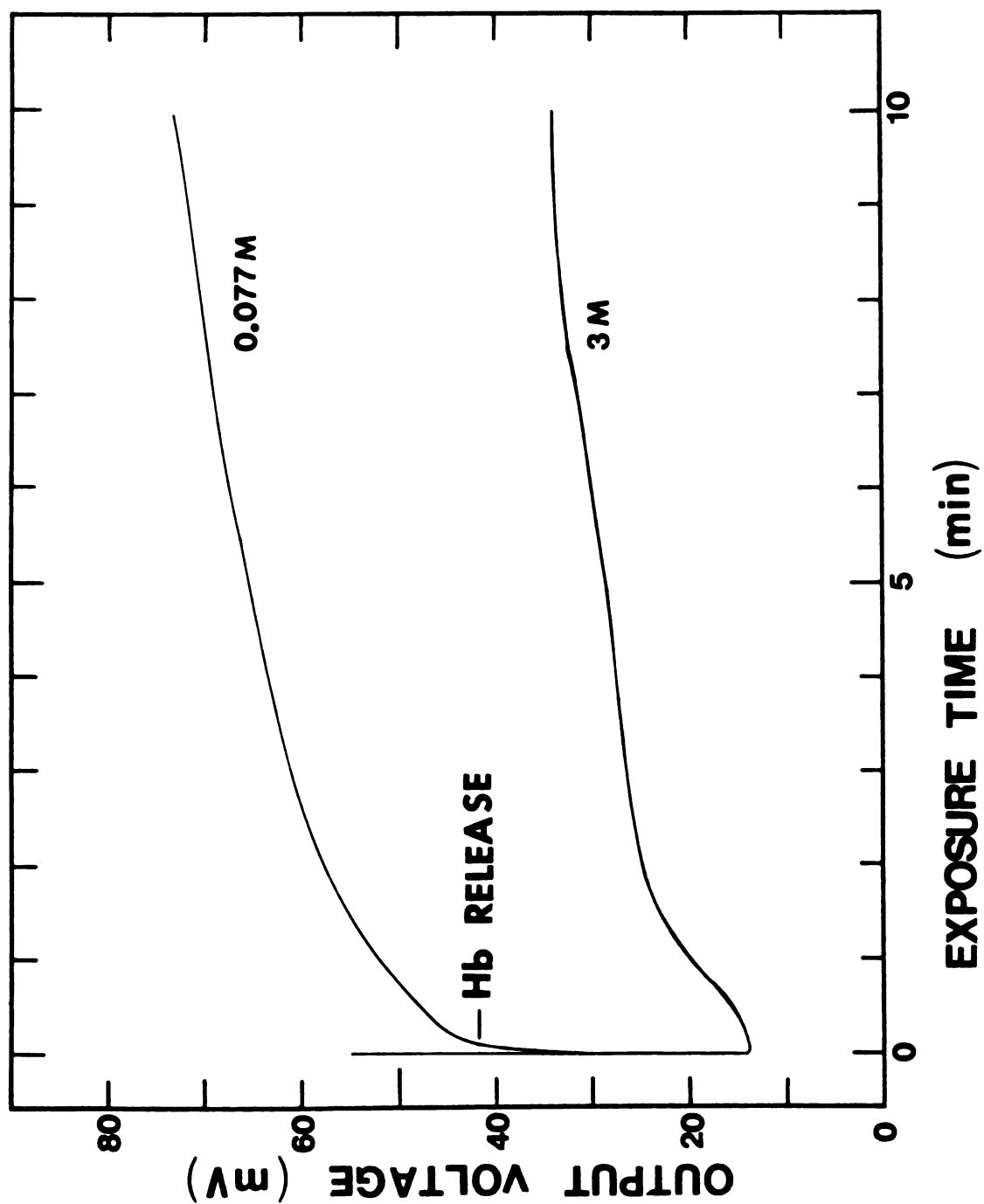


FIGURE 10.--Typical photocell voltage outputs as a function of exposure time.

time is much shorter than that of hypertonic-hemolysis. If the test solution NaCl concentration is less than 0.051 M, these zones of "rapid" and "smooth" signal changes actually overlap each other so that there is no discontinuity observed.

Hemolysis Kinetics of Erythrocytes

The hemolysis kinetics is established from the data by using the calibration curve (function) provided in Figure 6. The curves shown in Figure 11 represent the hemolysis kinetics under six different NaCl concentrations; three hypertonic and three hypotonic. Another three solutions, 1 M, 0.154 M (normal saline), and 0.102 M NaCl, were also tested. The results are not plotted since no significant hemolysis was observed within 10 minutes after mixing under these conditions. The curves shown are plotted as $\log (\% \text{ hemolysis})$ vs $\log (\text{exposure time})$. All curves were obtained from the same batch of cells which were prepared under identical conditions and subjected to the specified test solutions. Each curve represents an average of at least three consecutive experiments of the same test solution. The experimental error was about 2% to 5% and was not plotted. Larger variations were observed when cells from different batches were compared. But these results are not reported since this effect was not thoroughly investigated. Both hypertonic and hypotonic hemolysis reveals a rapid lysis rate, followed by a slower rate, and eventually the damage reaches a plateau which represents the steady-state hemolysis level. Cells are completely hemolyzed when subjected to mixing in test solutions with NaCl

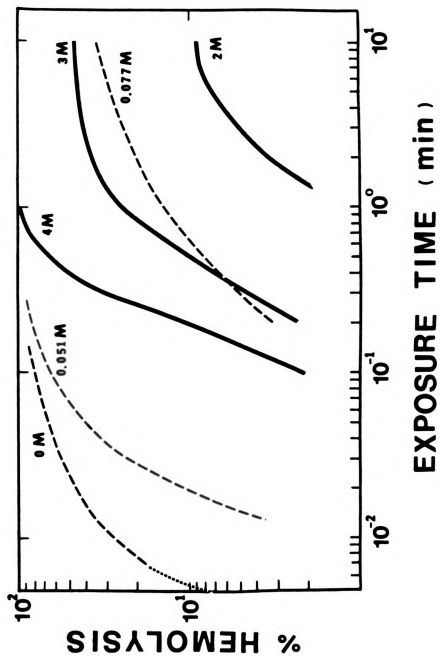


FIGURE 11.--Hemolysis kinetics at ambient temperature.

concentrations of 4 M, 0.051 M, and 0 M (distilled water). Both the steady state hemolysis value and the initial hemolysis rate increased as the test solution osmolarity deviated from that of the normal saline.

Since the present device provides a unique way to obtain information concerning the short time hemolysis data, which are important for hemolysis modeling (5), an analysis of this initial hemolysis is presented. Two parameters were chosen to quantify the initial hemolysis, namely, the reciprocal of lag time ($1/t_l$) and the initial rate of hemolysis (% hemolysis/minute). According to the calibration curve, 5% hemolysis yielded a \bar{V} of 1.066, which could be clearly distinguished from the background noise level. Consequently the lag time was defined as the time taken to induce 5% hemolysis. Characterizing the initial hemolysis rate as the % hemolysis divided by the exposure time can present problems due to the non-linearity of the hemolysis kinetics. First, if the time interval chosen was very short, the "initial rate" would be distorted by the existence of the lag time and their values would be underestimated. Second, if the time interval chosen was very long, the "initial rate" would become the "average rate" instead. Therefore, for the purpose of comparison the initial rate was defined as the hemolysis rate between 5% and 10% hemolysis. Both rate parameters are plotted as a function of the relative water activity and shown in Figure 12. The relative water activity, A_w/A_w^0 , where A_w is for the hypertonic or hypotonic case and A_w^0 is

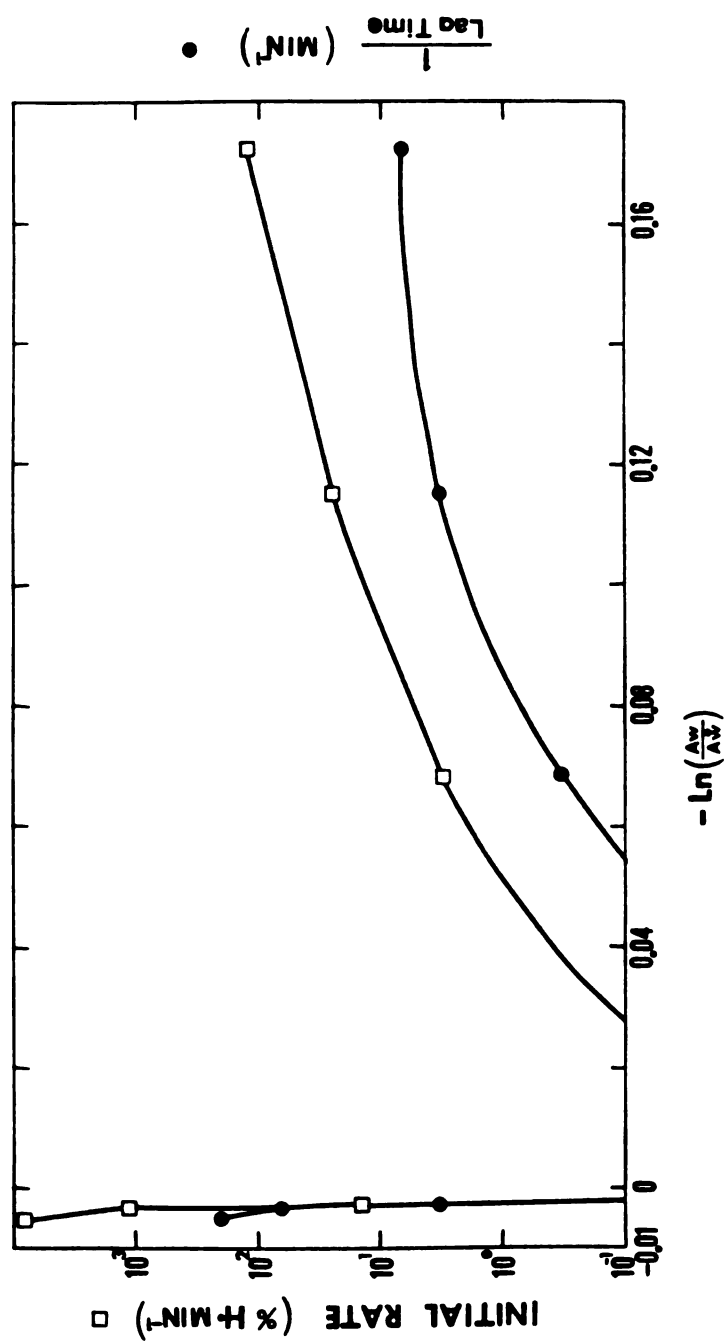


FIGURE 12.--Correlations of initial hemolysis rate as a function of water activity.

for the isotonic case, has been corrected for extracellular saline included in the "packed cell" sample. For example, one ml of packed cell (e.g., 86% hematocrit) was mixed with 9 ml of test solution (X M). The initial extracellular NaCl concentration, right after the mixing, was

$$\frac{(1-86\%) \cdot 0.154 + 9 \cdot X}{(1-86\%) + 9} = X'$$

The corrected molarity was then converted into water activity from reference 14.

The results in Figure 12 indicate that cells are relatively stable within the range of $-\ln(A_w/A_w^o)$ from -0.002 to +0.03. Beyond this range, cells exhibited detectable hemolysis within the observed experimental time period. It is very obvious that cells are much more sensitive to the hypotonic exposure than to hypertonic exposure. Minute alterations of the hypotonic test solution affect the hemolysis process dramatically. On the other hand, the initial portion of hemolysis kinetics is relatively unaffected by the perturbations of hypertonic test solution. If these curves in Figure 12 are extrapolated to the point where $-\ln(A_w/A_w^o) = 0$, i.e., $A_w = A_w^o$, the "stable time" of erythrocytes suspended in normal saline could be estimated. The values obtained were of the order of 10^4 minute, which is 7 days, for the lag time and 10^{-3} %hemolysis/minute, which is 1.4% hemolysis/day, for the initial rate of hemolysis. More data points are necessary if a good estimate is desired. However,

these rough estimates were consistent with the fact that the average life span of human red blood cells in vivo is about 120 days.

The Effect of Shear on Hemolysis

Since the injection process was manually performed, the stop flow injection flow rates were semi-quantitatively grouped into three ranges: slow, medium (routinely used), and fast injections. The injection times were estimated to be 1 second, 0.56 second, and 0.32 second respectively, from the traces on the recorder chart. With the known injection volume, the mean volumetric flow rate was calculated. Consequently, the Reynolds number was derived as follows, for various areas of the stop flow system in order to characterize the nature of the flow in its major parts.

$$Re_d = \frac{\bar{v} d \rho}{\mu}$$

where \bar{v} is the mean velocity in the tube (= volumetric flow rate/tube cross section area), ρ is the density of the cell suspension (about 1 g/ml), d is the tube diameter, and μ is the viscosity of the cell suspension. The results are presented in the table on the following page.

There is no simple model describing the flow conditions in the mixer. However, since the flow rate ratio of the packed cells to that of the test solution was 1:9, a flow pattern similar to that in Figure 13 (provided by Dr. J. F. Foss, Mechanical Engineering Department, Michigan State University) was suggested. In this figure, the test solution flows in the y-direction and the packed

	Tube Diameter (cm)	Hematocrit	Viscosity* (cp)	Flow Rate (ml/sec)	Mean Velocity (cm/sec)	Re _d
Blood Tube	0.1	85%	40	0.3 0.54 0.94	38.2 68.8 119.7	9.6 17.2 29.9
Test Solution Tube	0.1	0%	1	2.7 4.9 8.5	344 624 1080	3440 6240 10800
Test Chamber	0.32	8.5%	1.6	3.0 5.4 9.4	37.3 67.1 116.9	746 1340 2240

*The hematocrit dependent viscosity was obtained from reference (15).

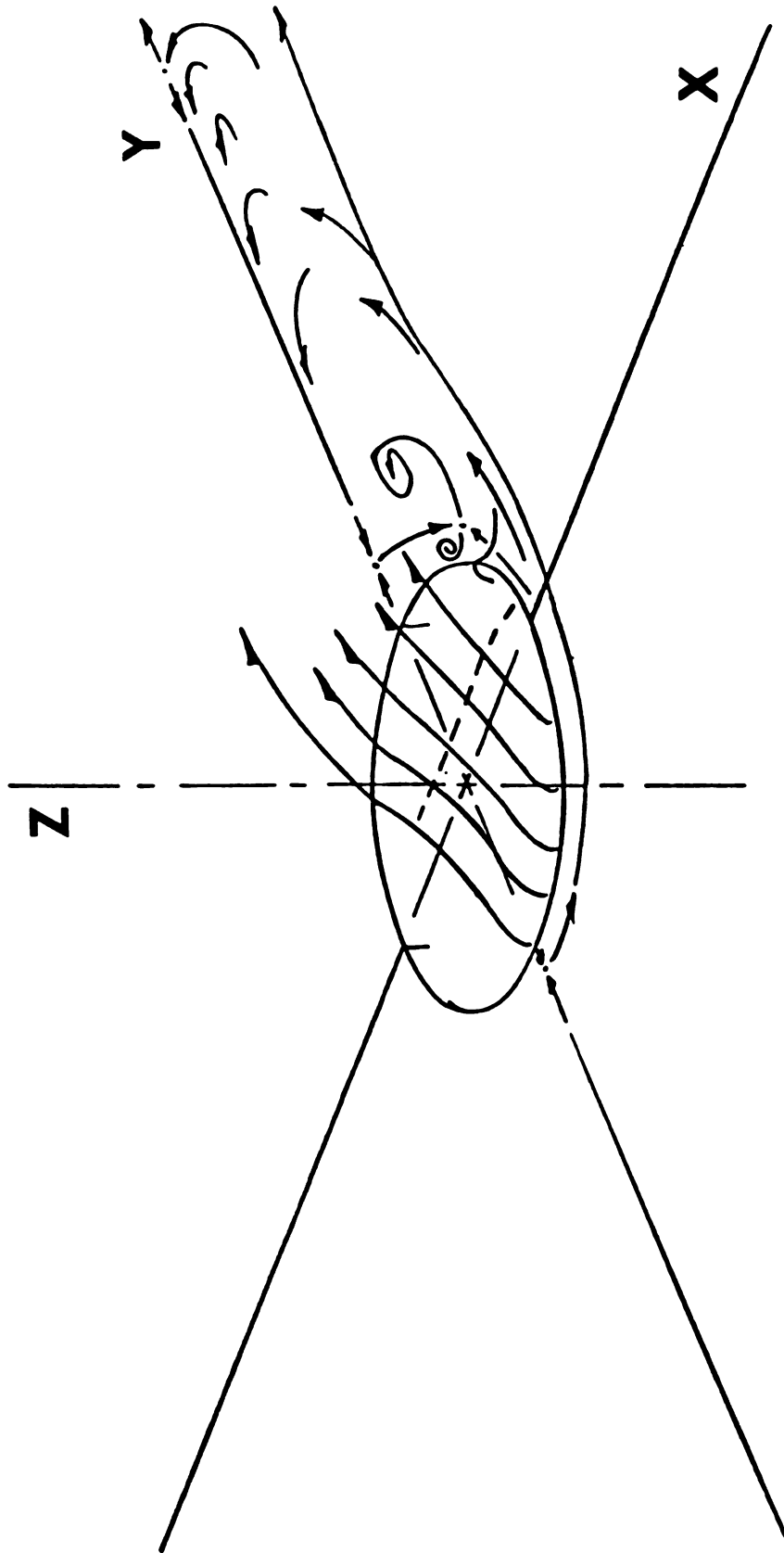


FIGURE 13.--Proposed flow pattern in the mixer.

cells flows in the z-direction. In general, a turbulence was formed behind the blood injection point and spread to the rest of the mixer.

The final flow in the test chamber was probably turbulent because (a) the Reynolds number in the test solution tube was high enough for turbulence, (b) the flow in the mixer was turbulent and was likely to propagate into the test chamber, and (c) the blood flow in capillary tubes was reported to demonstrate turbulent transition when $Re_d > 800$ (16). Unfortunately, there is no existing information about the Reynolds number at which turbulence occurs for tubes of the size (and surface properties) as the currently used test chamber.

The hemolysis kinetics as a function of different flow rates is shown in Figure 14, where o: slow injection, ● medium injection, Δ: fast injection, solid line: hypertonic exposure, broken line: hypotonic exposure. Hypotonic (0.077 M NaCl) hemolysis took place faster and was more severe when flow rate increased. On the other hand, there was no apparent influence of shear, within the experimental flow-rate range, on the hemolysis kinetics when cells were exposed to hypertonic solution (3 M NaCl).

The Effect of Storage Time on Hemolysis Kinetics

Red blood cells generally have a life span of approximately 120 days in vivo (2). However, the life span in vitro is generally considerably shorter. Blood samples are stored in blood banks for a maximum of 21 days before the transfusion is carried out. Long term non-freezing storage is not yet available because of possible

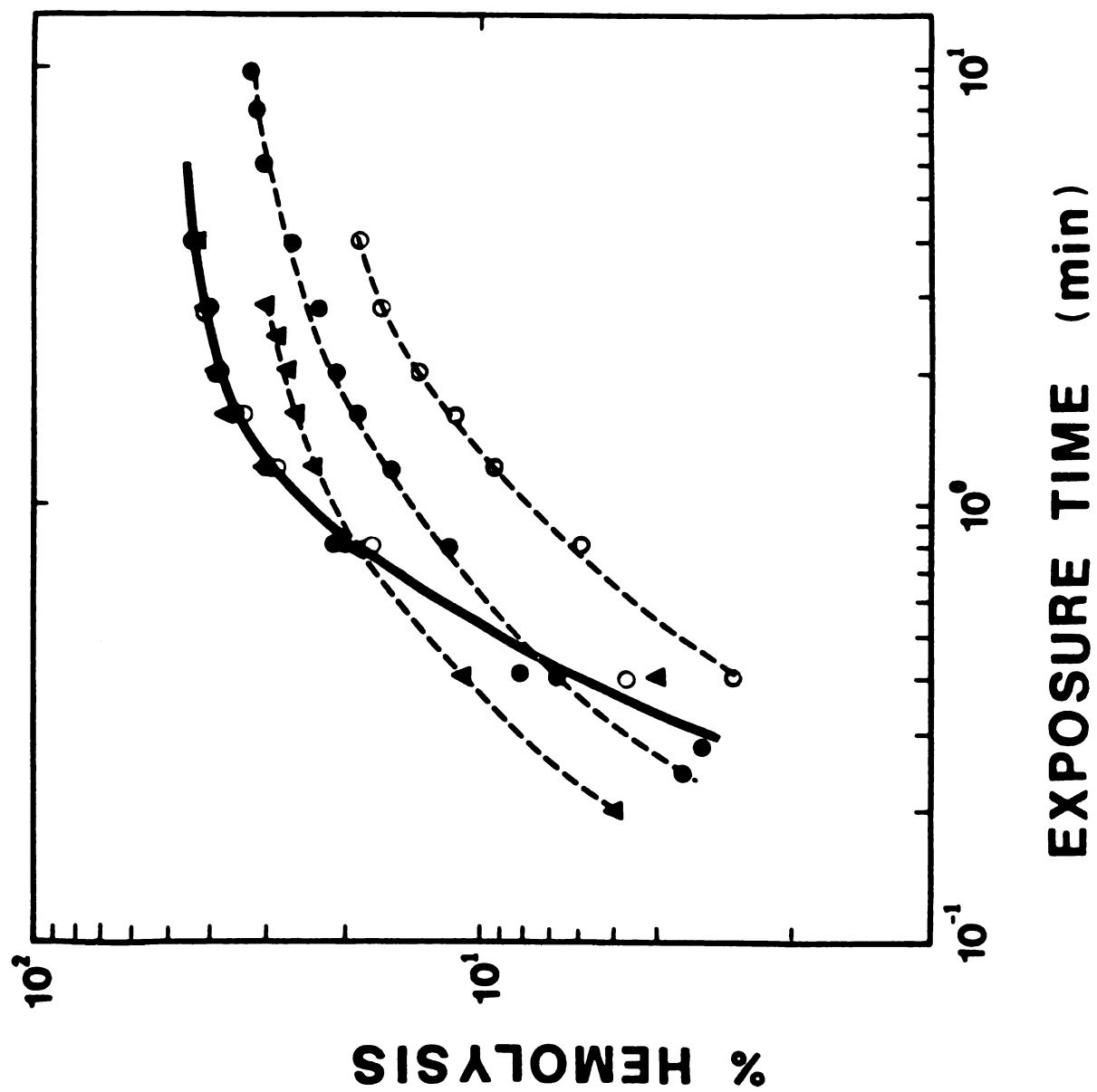


FIGURE 14.--Effect of injection rate on hemolysis kinetics.

cellular damage. Cells of different storage time do show hemolysis kinetics which are different from non-stored cells (Figure 15).

"Aged" cells were more fragile with respect to both hypertonic and hypotonic perturbations. The steady state hemolysis value increases with storage time. For cells subjected to hypertonic exposure (3 M NaCl), the initial rate of hemolysis is relatively insensitive to storage time. On the other hand, the initial rate of hemolysis due to hypotonic exposure (0.077 M NaCl) increases about 20-fold within the first 5 days of storage. Since some of these already-hemolyzed cells were presumably removed during the washing procedure, the actual storage effect on hemolysis kinetics might be even more dramatic than that which is presented.

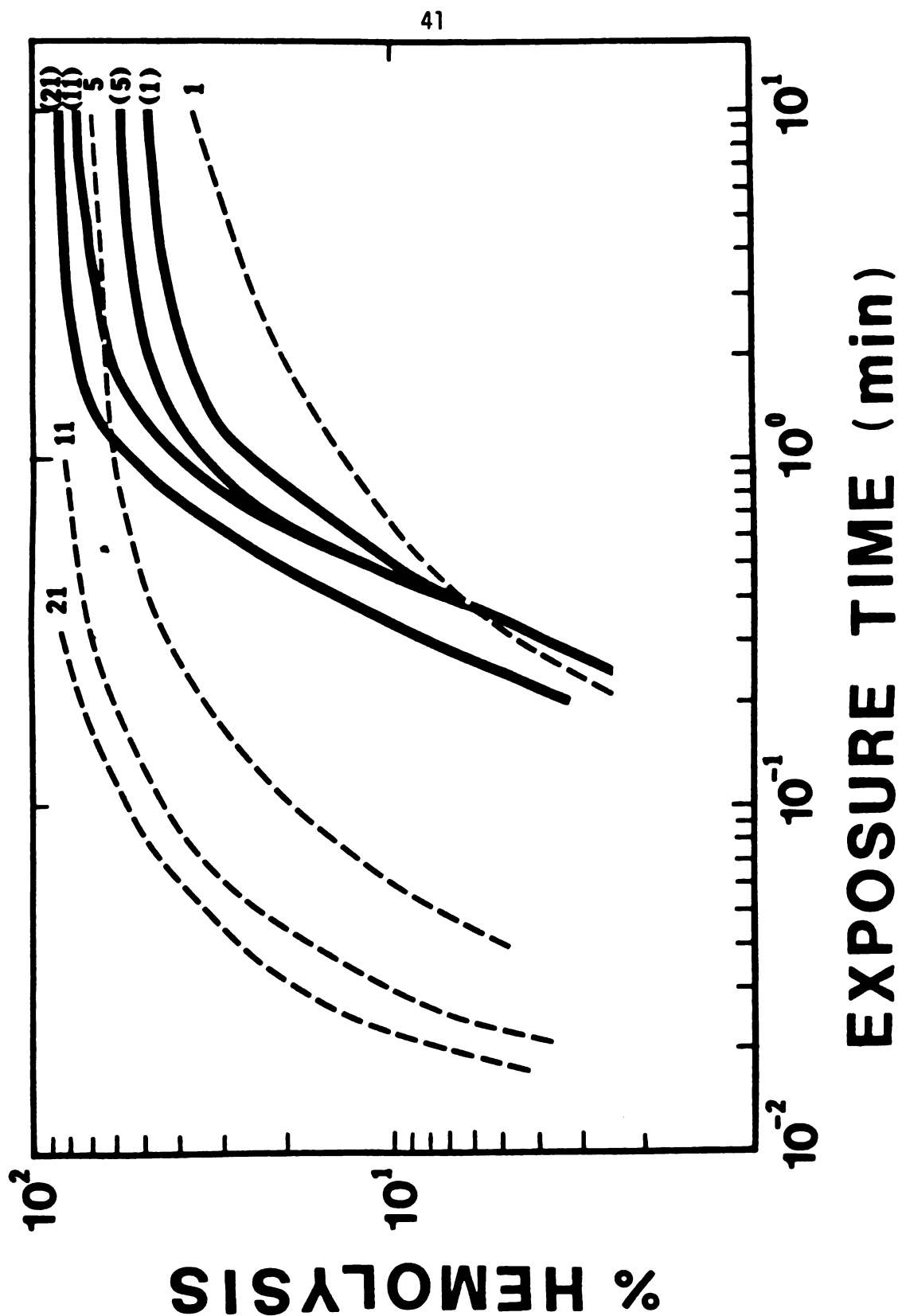


FIGURE 15.--Effect of blood storage time on hemolysis kinetics.

CHAPTER V

DISCUSSION

An experimental apparatus and technique have been developed, which allow the determination of hemolysis kinetics on a real-time basis for a wide range of osmotic perturbations. Because of the thorough mixing and the geometry of the system, the hemolysis data can be obtained with a maximum dead time of approximately 0.2 second. This technique offers a convenient method of measuring the initial rate of hemolysis, especially when cells are subjected to severe osmotic perturbation and the hemolysis process is essentially completed within several seconds. This is an important feature of the present technique since it makes short time experimental data accessible for characterization and modeling.

Since the results indicate that the hemolysis kinetics are flow-rate dependent, the current injection system should be improved in the future. A pressure-controlled drive would provide a desired injection rate and hence more reproducible results which appears to be particularly important in the area of hypotonically induced damage. Moreover, a more quantitative analysis of the shear effect on hemolysis kinetics can then be obtained by carefully adjusting the injection rate and analyzing the shear in the system. Experiments with turbulent flow conditions also generate valuable

information since the in vivo blood flow is turbulent around the heart valves and the first major branches in the arterial system (17,18). As mentioned earlier in this presentation, a complete and rapid mixing of cells with the test solution can only be achieved by having sufficiently high injection rates, which may induce undesired mechanical damage to the cells. With the help of data from studies on the quantitative shear effect on hemolysis, the osmotic perturbation induced hemolysis can be decoupled from the shear-induced hemolysis and analyzed independently. Alternatively, a thin chamber in which the mixing process is achieved by the diffusion of test solution through filters or semipermeable membranes could be constructed to minimize the shear effect. However, access to the data of rapid kinetics may be sacrificed by using this "diffusion chamber," if it is too thick.

As compared to the earlier designs of this kind the present apparatus and procedures offer an important advantage, i.e., the optical transients (artifacts) observed after the flow is stopped are largely removed. In order to understand the possible mechanisms involved in the artifact, the following relevant information and facts are presented: (a) optical transients are only observed when the cell suspensions are subjected to flow; (b) upon cessation of flow, the optical transients decay in about 30 seconds under most experimental conditions; (c) the magnitude and time scale of these transients apparently do not depend on the configuration of the apparatus. These facts are a result of work in reference (5,11,19) and several different mixers and test chambers tested by the author.

(d) The transients are also seen either when an isotonic cell suspension is mixed in the stop flow with the same type of isotonic cell suspension (11), or when a single cell suspension is directly injected into the test chamber without mixing with any other solution. Therefore, neither the dilution effect nor the mixing effect can account for the results. (e) The phenomenon is critically dependent on red cell shape. Cells transformed from disc to sphere by aging, detergents, low salt concentrations, or metabolic depletion demonstrate reduced optical transients (11,19,20). (f) Glutaraldehyde fixed cells (rigid cells) also show optical transients (20). (g) Cells carried in a flow field have statistically preferred orientations (21,22). The light transmission is cell orientation-dependent (20), whereas the light scattering is detector angle-dependent (19,23).

Based on the above information the author proposes the following mechanism of optical transients. (a) Asymmetrically shaped cells are aligned in a flow field and hence transmit more light than the disordered cell suspension. (b) The gradual decrease of signal level (artifact) is due to the random motion of cells after flow cessation. Then the question becomes why these optical transients are reduced by increasing cell density (hematocrit) as observed in Figure 8. The apparent viscosity does not change significantly as a result of a change in hematocrit from 2% to 10% (15), and hence should not change the flow pattern dramatically. Although cells in higher hematocrit (50%) suspensions are "better aligned" in the capillary tube as compared to those in lower (1%)

hematocrit suspensions (24), this probably does not apply to our test chamber which has an inner diameter of 0.32 cm. On the other hand, if a high hematocrit condition does show better alignment of the cells in the flow, the optical transients should be enhanced, which is contradictory to the experimental results. Therefore, the author interprets the hematocrit effect on the optical transients as follows: (a) The magnitude of optical transients is reduced by multiple scattering within the cell suspension when its hematocrit is high. (b) The frequency of cell-cell collision after the flow is stopped is enhanced by higher hematocrit conditions. As a consequence, the reduced optical transients damp out very quickly. An estimate of a Brownian motion characteristic time (t_B) for randomization of erythrocyte orientation is calculated based on the model provided in reference (25).

$$R_\omega = (\kappa T) t_B,$$

where the quantity R_ω is the ratio of torque required to rotate the particle divided by the resulting angular velocity, κ is Boltzmann's constant. For a disc-shaped particle,

$$R_\omega = \frac{32}{3} R^3 \mu,$$

where R is the radius of the particle and μ is the suspension viscosity. The calculated t_B is about 160 seconds for an erythrocyte in a collision-free suspension. This interpretation is further supported by the fact that optical transients of scattered light

from diluted cell suspension (about 0.5% hematocrit) could be as high as 100% of the initial signal value and lasted as long as 2-3 minutes (19).

Since the experiments quantifying the artifact (Figure 8) were performed by injecting pre-mixed samples into the test chamber, the cells were probably aligned by the flow under these conditions. On the other hand, if the mixer which generates the turbulent flow is applied, the cells might be more randomly oriented so that the magnitude of the optical transients are much more reduced even when low hematocrit samples are used. Thus this hypothesis could be tested easily.

It is the author's experience that results from the same batch of cells are very reproducible, whereas larger deviations are observed by comparing samples collected on different days by the blood bank. Two possibilities could account for this: (a) samples from different donors are different and (b) samples might be collected and handled differently from day to day. Using fresh blood from one single donor, collected in citrate phosphate buffer instead of EGTA tubes, should improve the reproducibility.

Perhaps the most serious source of systematic error in this technique is the calibration curve (Figure 6). The correlation of \bar{V} to %hemolysis is established by measuring partially hemolyzed samples in normal saline. Two assumptions are made in order to use this correlation as a calibration: (a) there is no significant cellular damage induced by the centrifugation process in determining

the %hemolysis and (b) the same correlation holds for both hypotonic and hypertonic experimental conditions.

Red cells suspended in isotonic saline do not give significant hemolysis by spinning in a clinical centrifuge. Therefore, the first assumption holds under current experimental procedures in obtaining the calibration curve. On the other hand, the hemolysis process induced by osmotic exposure is believed to be preceded by cell volume changes which alter the light transmission and scattering properties of the pre-hemolyzed cell suspension. Theoretically one should construct a calibration curve for each test solution. However, it is practically too difficult to do so, especially for cells undergoing very rapid hemolysis when subjected to severe osmotic shock. Another approach is to construct two calibration curves, one for hypertonic hemolysis and the other for hypotonic hemolysis. $V_{0\%H}$ is defined as the signal values from cells at hypotonic and hypertonic critical volumes respectively. But the cells at critical volumes are very fragile and hence may be hemolyzed by even very small perturbations generated in the measurement procedure, e.g., centrifugation. In conclusion, the current methods in obtaining the calibration curve are convenient, but one should always keep the shortcomings in mind while presenting the hemolysis kinetics quantitatively.

Suggestions for Future Work

Hemolysis kinetics data, especially the hypertonic hemolysis portion, are certainly useful in understanding the mechanisms of

freeze-thaw injury (5). For a complex process like freezing, which involves simultaneous variations in both temperature and concentration, quantitative prediction of total damage is impossible unless one has the knowledge concerning how these two modes are coupled. The current technique enables the monitoring of the osmotic mode of damage. By performing the same experiments at different temperatures one should be able to access the thermal mode of damage as well. Furthermore, the precise measurements of initial rate and lag time of the hemolysis process will help determine the accuracy of theoretical thermodynamic rate equations (5).

Evidence in the literature suggests that hemolysis produced by osmotic shock is accompanied by the loss of various membrane components (8,26). The release of membrane components in a non-equilibrium process was considered as the possible mechanism of hemolysis (5). Preliminary results obtained by the author do show alterations of hemolysis kinetics from cells subjected to different numbers of wash, which is known to remove various cell membrane components (8). More detailed studies of this kind should be helpful in verifying this proposed mechanism of hemolysis.

When blood is stored in liquid medium, a series of biochemical changes that influence the viability of stored cells occurs (27). The first important change consists of a sharp drop in 2,3-diphosphoglyceric acid (2,3DPG) levels. The level of 2,3DPG within the red cell is an important determinant of hemoglobin function. Secondly, the concentration of ATP falls and the red cells lose the ability to phosphorylate glucose, and the sodium-potassium pump

breaks down. Potassium leaks from the cell and sodium gains entry into the cell. As a result the osmotic fragility of stored red cells is increased and some undergo spontaneous lysis. The hemolysis kinetics induced by hypotonic exposure changes dramatically within the first 5 days of storage (Figure 15). Interestingly, it is also reported that the 2,3DPG level drops down to 20% of normal level within the same storage time period (28). Therefore, it would be very useful to investigate the possibility that the cell fragility is indeed regulated by the cellular hemoglobin and/or energy state.

Aging, diseases (hemolytic anemia, sickle cells, etc.), chemicals (acetic acid, alcohols, cholesterol, etc.) and contact with material surfaces will all influence the behavior of red blood cells. Some of these factors will change the cell shape, other change the cell volume or membrane components. Most of these alterations will be reflected as changes of the cell fragility. Hemolysis kinetics measurements of these samples can be invaluable in quantifying the effect of various factors and hence understanding the possible mechanisms causing them.

REFERENCES

1. Castle, W. B. Disorders of the blood. In Sodeman, W. A. (ed.), "Pathological Physiology: mechanisms of disease," 3rd ed. p. 889, (1961).
2. Ponder, E. "Hemolysis and Related Phenomena," p. 90 (1948).
3. Zade-Oppen, A. A. M. Posthypertonic hemolysis in sodium chloride systems. *Acta Physiol. Scand.* 73, pp. 341-364 (1968).
4. Mazur, P., S. P. Leibo and R. H. Miller. Permeability of the Bovine red cell to glycerol in hyperosmotic solutions at various temperatures. *J. Memb. Biol.* 15, pp. 107-136 (1974).
5. McGrath, J. J. The kinetics and thermodynamics of human erythrocyte freeze-thaw damage at sub-optimal colling rates. Ph.D. thesis, MIT (1977).
6. Mazur, P., S. P. Leibo, J. Farrant, E. H. Y. Chu, M. G. Hanna and L. H. Smith. Interactions of cooling rate, warming rate and protective additive on the survival of frozen mammalian cells. In "The Frozen Cell" pp. 69-88 (1970).
7. Lovelock, J. E. The hemolysis of human red blood cells by freezing and thawing. *Biochem. Biophys. Acta* 10, pp. 414-426 (1953).
8. Lovelock, J. E. The physical instability of human red blood cells. *Biochem. J.* 60, pp. 692-642 (1955).
9. Anderson, N. M. and P. Sekelj. Light-absorbing and scattering properties of non-hemolyzed blood. *Phys. Med. Biol.* 12, pp. 173-184 (1967).
10. Kermack, W. O., A. G. McKendrick and E. Ponder. The stability of suspensions III. the velocities of sedimentation and of cataphoresis of suspensions in a viscous fluid. *Proc. Roy. Soc. Edinburgh* 49, pp. 170-197 (1929).
11. Papanek, T. H. The water permeability of human erythrocyte in the temperature range +25 °C to -10 °C. Ph.D. thesis, MIT (1978).

12. Farrant, J. and A. E. Woolgar. Human red cells under hypertonic conditions: a model system for investigating freezing damage: 1. sodium chloride. *Cryobiol.* 9, pp. 9-15 (1972).
13. Saari, J. T. and J. S. Beck. Hypotonic hemolysis of human red blood cells: a two-phase process. *J. Memb. Biol.* 23, pp. 213-226 (1976).
14. Robinson, R. A. and R. H. Stokes. "Electrolyte Solutions." Butterworths, p. 476 (1970).
15. Cokelet, G. R. The rheology of human blood. In Fung, Y. C., Perrone, N., and Anliker, M. (eds.) "Biomechanics: Its Foundation and Objectives" pp. 63-103 (1972).
16. Merrill, E. W., E. R. Gilliland, G. Cokelet, H. Shin, A. Britten and R. E. Wells Jr. Rheology of blood: temperature and hematocrit effects. *Biophys. J.* 3, 199-213 (1963).
17. Whitmore, R. L. "Rheology of the Circulation" (1968).
18. Cooney, D. O. "Biomedical Engineering Principles: an introduction to fluid heat, and mass transport processes," pp. 73-74 (1976).
19. Oster, G. and R. Zalusky. Shape transformation of erythrocytes determined by light scattering changes associated with relaxation of particle orientation. *Biophys. J.* 14, pp. 124-129 (1974).
20. Frojmovic, M. M., A. Okagawa and S. G. Mason. Rheo-optical transitions in erythrocyte suspensions. *Biochem. Biophys. Res. Comm.* 62, pp. 17-24 (1975).
21. Burton, A. C. "Physiology and Biophysics of the Circulation" (1965).
22. Lightfoot, E. N. "Transport Phenomena and Living Systems" (1974).
23. Latimer, P. and B. E. Pyle. Light scattering at various angles: theoretical predictions of the effects of particle volume changes. *Biophys. J.* 12, pp. 764-773 (1972).
24. Goldsmith, H. The microrheology of red blood cell suspensions. *J. Gen. Physiol.* 52, pp. 5s-27s (1968).
25. Lightfoot, E. N. "Transport phenomena and living systems" pp. 433-434 (1974).

26. Lovelock, J. E. The denaturization of lipid-protein complexes as a cause of damage by freezing. Proc. Roy. Soc. Ses. B., 147, pp. 427-433 (1957).
27. Wintrobe, M. M. "Clinic Hematology." 7th ed. (1974).
28. Bunn H. F., and J. H. Jandl. Control of hemoglobin function within the red cell. New Engl. J. Med. 282, p. 1414 (1970).